Magnetism of amorphous carbon nanofibers

S. Ma,[1,2] J. H. Xia,[1] Vadali V. S. S. Srikanth,[1,a)] X. Sun,[1] T. Staedler,[1] X. Jiang,[1,b)] F. Yang,[2] and Z. D. Zhang[2]
[1]*Institute of Materials Engineering, University of Siegen, Paul-Bonatz-Str. 9-11, 57076 Siegen, Germany*
[2]*Shenyang National Laboratory for Material Science, Institute of Metal Research, and International Centre for Material Physics, Chinese Academy of Sciences, 72 Wenhua Road, Shenyang 110016, People's Republic of China*

(Received 27 August 2009; accepted 18 November 2009; published online 30 December 2009)

Amorphous carbon nanofibers (ACNFs) have been synthesized by a thermal chemical vapor deposition technique. The ACNFs grow as two branches perpendicular to {111} facets of a catalytic copper nanoparticle. The carbon nanofibers are composed of disordered localized nanofragments which in turn consist of several graphene layers. The ACNFs show a paramagnetic characteristics at 2, 5, and 10 K. The magnetic moments are suggested to originate from a large amount of defects in the graphene layers of the nanofragments. © *2009 American Institute of Physics*. [doi:10.1063/1.3272940]

The discovery of ferromagnetism in polymerized C_{60},[1,2] has led to similar findings in other carbon nanomaterials, namely, nanographite,[3] nanofoam,[4] nanospheres,[5] and nanodiamond[6] which are zero-dimensional. However, when it comes to applications, only one-dimensional (1D) materials can facilitate carbon-nanostructures-based magnetic-device assembling. In this context, a kind of pitch-based activated carbon fibers (ACFs) with a diameter of 10 μm have been synthesized.[7] However, these ACFs only show antiferromagnetic behavior at 2 K,[8] which has less possibility to be applied in the design of nanodevices. For synthesizing useful 1D carbon materials, such as paramagnetic or ferromagnetic carbon nanomaterials, carbon nanofibers with optimized structure should be designed. In this letter, we present the paramagnetic characteristics of a unique class of 1D carbon nanostructures which we name amorphous carbon nanofibers (ACNFs). These ACNFs are expected to be promising candidates in nanodevice designing. It is also expected that they will generate new research interest with regard to magnetism in the carbon-based 1D nanomaterials and that further modified nanostructures may show ferromagnetic characteristics.

The ACNFs were synthesized by a thermal chemical-vapor-deposition technique.[9] Copper tartrate (dispersed on a copper substrate) and acetylene were used as reaction precursors. The reaction temperature, reaction-gas pressure, and annealing temperature were 523 K, 500 mbar, and 1173 K, respectively. Structural and phase analysis of the ACNFs was carried out by scanning electron microscopy (SEM), transmission electron microcopy (TEM), x-ray diffraction (XRD) with Cu-K_α radiation, and micro Raman scattering with a laser wavelength of 532 nm. The magnetic behavior of the ACNFs was studied by using a superconducting quantum interference device. Before the measurements, the ACNFs were washed two to three times with 2M HNO_3 for removing ferromagnetic-metal impurities, if any.

The SEM image [Fig. 1(a)] shows the morphology and distribution of the ACNFs. It can be observed that the length of the individual ACNFs is at least 10 μm while the diameter distribution ranges from 150 to 300 nm. The TEM image [Fig. 1(b)] presents the two-branches feature of the ACNFs. It can be observed that two nanofibers have simultaneously grown perpendicular to two facets of the catalyst nanoparticle [darker-contrast part in Fig. 1(b)]. It can also be seen that the diameter of the fiber is about the same as the size of the catalyst. The selected area electron diffraction (SEAD) pattern of one ACNF indicates the crystalline characteristic of the two nanofibers and the catalytic particle [Fig. 1(c)]. In the SEAD pattern, the single-crystal-diffraction pattern of a Cu nanoparticle with $[10\bar{1}]$ zone axis is seen. The two carbon nanofibers grow on two {111} facets of the Cu particle and the growth direction of the carbon fiber is along the ⟨111⟩ direction of the copper nanoparticles. On the other hand, no typical diffraction ring for amorphous carbon is observed in the SAED pattern, while two elongated diffraction spots in the ⟨111⟩ direction of copper suggest that the carbon nanofibers are crystalline along the ⟨111⟩ direction of the copper nanoparticle.

The powder XRD pattern, shown in Fig. 2, presents the phase composition of the ACNFs. The broad reflection at 24.1° indicates the amorphous nature of the ACNFs. The other four peaks indicate the existence of fcc Cu and the

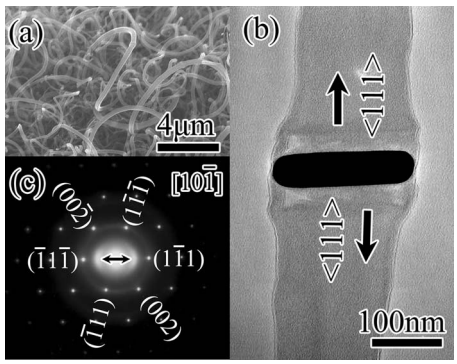

FIG. 1. (a) Low-magnification SEM plane view image of ACNFs, (b) TEM plane view image of a representative ACNF, and (c) the SAED of the ACNF shown in (b).

a)Present address. School of Engineering Sciences and Technology, University of Hyderabad, Central University, Hyderabad, India 500046.
b)Author to whom correspondence should be addressed. Electronic mail: xin.jiang@uni-siegen.de.

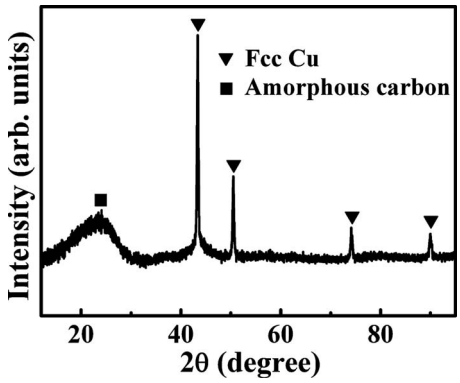

FIG. 2. XRD pattern of the ACNFs.

absence of any other phases (for example, metallic impurities) in the sample.

The Raman spectrum (Fig. 3) reveals the structure of the carbon nanofibers in ACNFs. Two distinct peaks of 1345 and 1580 cm^{-1} are assigned to the D and G band of graphitic material, respectively. The G band has sp^2 content indicating the crystalline graphite, while the D band has sp^3 content indicating the disorder modes induced by defects (vacancies).[10] The broad G peak with full width at half maximum (FWHM) of 75.34 cm^{-1} indicates that the carbon nanofibers are constructed by the graphitic fragments with smaller grain sizes, because the value of FWHM is much larger than 12 cm^{-1} for graphitic samples with a large grain size.[7,10,11] The average size of the graphitic fragments can be further estimated from the intensity ratio of D and G bands. The in-plane crystallite size (L_α) of the graphitic fragment can be calculated by the function $L_\alpha(\text{nm}) = C \times (I_G/I_D)$.[12] The coefficient C was calculated by the function $C(\lambda_L) \approx C_0 + \lambda_L C_1$, where C_0 and C_1 were estimated to be -12.6 and 0.033 nm.[12] In this way, values of C (λ_L=532 nm) and I_G/I_D were calculated equal to 1.37 and 4.956, and the average size L_α of the graphitic fragments was estimated to be 6.79 nm. Therefore, according to the above Raman and XRD analysis, it can be inferred that the structure of the ACNFs is constituted by disordered localized nanofragments, while each nanofragment in turn consists of several graphene layers with a large amount of defects (vacancies). The structural schematic image of an amorphous carbon nanofiber is shown in the inset of Fig. 3.

Figure 4(a) shows the field-cooled (FC) magnetization of a sample (catalyst Cu nanoparticles+carbon branches) at a

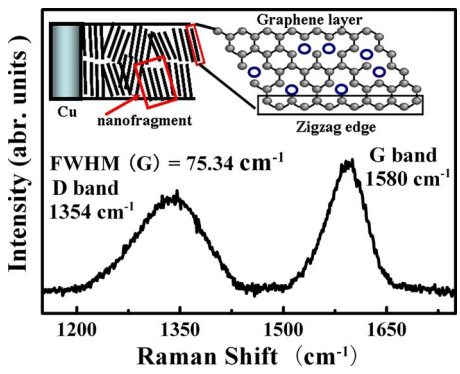

FIG. 3. (Color online) Raman spectrum of the ACNFs and schematic image of the carbon nanofiber in the inset.

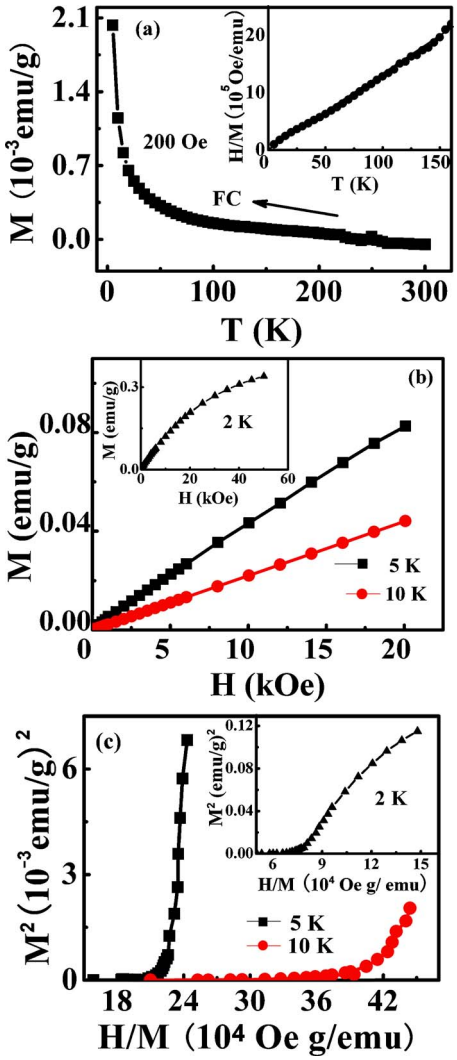

FIG. 4. (Color online) (a) FC M-T curve of ACNFs in a magnetic field of 200 Oe from 5 to 300 K and, in the inset, H/M vs T, (b) M-H of ACNFs at 5 K (triangles) and 10 K (circles) and, in the inset, M-H at 2 K, and (c) Arrott plots of ACNFS at 5 and 10 K and, in the inset, the Arrott plot at 2 K.

magnetic field of 200 Oe. The FC magnetization is positive below 200 K, as shown in Fig. 4(a). Having measured a positive magnetization for the sample, it is now important to determine the phase that is responsible for this. Only for copper nanoparticles with size below 5 nm and at temperatures below 560 pK, the magnetic behavior may change from diamagnetic to paramagnetic.[13,14] However, the copper nanoparticles in the present sample are larger than 150 nm as shown by the SEM and TEM results. This means that the copper nanoparticles in the present sample are diamagnetic at all temperatures [Fig. 4(a)]. Also, carbon (graphite and diamond) and copper in bulk form are typically diamagnetic. From this, it can be concluded that the ACNFs in the sample are responsible for the positive magnetization. The H/M versus T, i.e., χ^{-1} versus T, plot presented in the inset of Fig. 4(a) is linear at low temperatures and passes through the origin, exhibiting Curie-type of behavior. Because, at these low temperatures, the diamagnetism of Cu (-0.1×10^{-6} emu/g Oe) can be neglected compared to the large paramagnetic susceptibility, the observed Curie behavior of the susceptibility can entirely be attributed to the ACNFs.

The determination of the value of the initial susceptibility from the almost linear M-H curves at 5 and 10 K [Fig.

4(b)] is straightforward. Because of the stronger curvature of the M-H curve at 2 K [inset of Fig. 4(b)], we have performed an Arrott-plot analysis to determine the value of the initial susceptibility at this temperature. Figure 4(c) presents the result (inset), together with the Arrott plots at 5 and 10 K. The Arrott plots clearly prove the paramagnetic behavior of the ACNFs at the temperatures investigated. In order to estimate the size of the magnetic moments involved, we have interpreted the nonlinear magnetization, measured at 2 K up to 50 kOe, in terms of the paramagnetic Langevin curve. After correcting for the diamagnetic contribution of the copper, the average moment of the carbon branch can be estimated to be about 0.6 μ_B per 1000 C atoms. If the average magnetic moment induced by one defect is around 2 μ_B (vacancies at different positions give rise to different moments),[15] it would suggest that there is about one defect on each 3000 atoms in the graphene layer.

Different from diamagnetic bulk graphite, the carbon branches of the ACNFs, with their structural units being nanofragments constructed by graphene layers, present paramagnetic characteristics. The magnetic moments may be related with the structural characteristics of the ACNFs. According to the Raman analysis above, a large amount of defects (mainly vacancies) exist in the graphene layers of the nanofragments. Thus, the carbon atoms neighboring to defects (vacancies) will adjust their bonds to accommodate the defects and produce a dangling sp^2 orbit, which generates a magnetic moment.[3,15–17] However, the magnetism of ACFs induced by defects is antiferromagnetism, while bulk graphite with defects is ferromagnetic.[16] Therefore, the magnetism of these graphitic materials, induced by defects, depends sensitively on the concentration and the distribution of the defects as well as on the local bonding environment.[15] According to electronic-structure calculations with density functional theory, the way to enhance the moments and to induce a ferromagnetic interaction in nanographite system includes H atoms attached to a zigzag edge and a combination of vacancy defects and impurities (H or N atoms).[3,4,15] For the present ACNFs, the edge of graphene layers is not completely zigzag-type, because of the existence of another type of edge, the armchair edge, which does not induce the ferromagnetism.[16] Therefore, control of the quantity and the distribution of defects in the nanofragments will be of prime importance in preparing ferromagnetic ACNFs.

In summary, by using the thermal chemical-vapor deposition technique, paramagnetic ACNFs have been synthesized. The moments of the ACNFs may originate from the defects (mainly vacant sites) in the graphene layer of the nanofragments.

This work was supported by Deutsche Forschungsgemeinschaft (Grant No. DFG JI22/3/JI22/7-2) and National Basic Research Program of China, Ministry of Science and Technology China (Grant No. 2010CB934603).

[1] P. Turek, K. Nozawa, D. Shiomi, K. Awaga, T. Inabe, Y. Maruyama, and M. Kinoshita, Chem. Phys. Lett. **180**, 327 (1991).
[2] R. Höhne and R. Esquinazi, Adv. Mater. **14**, 753 (2002).
[3] K. Kusakabe and M. Maruyama, Phys. Rev. B **67**, 092406 (2003).
[4] A. V. Rode, E. G. Gamaly, A. G. Christy, J. G. Fitz Gerald, S. T. Hyde, R. G. Elliman, B. Luther-Davies, A. I. Veinger, J. Androulakis, and J. Giapintzakis, Phys. Rev. B **70**, 054407 (2004).
[5] D. Li, Z. Han, B. Wu, D. Y. Geng, and Z. D. Zhang, J. Phys. D: Appl. Phys. **41**, 115005 (2008).
[6] E. M. Levin, X. W. Fang, S. L. Bud'ko, W. E. Straszheim, R. W. McCallum, and K. Schmidt-Rohr, Phys. Rev. B **77**, 054418 (2008).
[7] A. M. Rao, A. W. P. Fung, M. S. Dresselhaus, and M. Endo, J. Mater. Res. **7**, 1788 (1992).
[8] Y. Shibayama, H. Sato, and T. Enoki, Phys. Rev. Lett. **84**, 1744 (2000).
[9] Y. Qin, X. Jiang, and Z. L. Cui, J. Phys. Chem. B **109**, 21749 (2005).
[10] A. C. Ferrari and J. Robertson, Philos. Trans. R. Soc. London, Ser. A **362**, 2477 (2004).
[11] O. E. Andersson, B. L. V. Prasad, H. Sato, T. Enoki, Y. Hishiyama, Y. Kaburagi, M. Yoshikawa, and S. Bandow, Phys. Rev. B **58**, 16387 (1998).
[12] M. J. Matthews, M. A. Pimenta, G. Dresselhaus, and M. Endo, Phys. Rev. B **59**, R6585 (1999).
[13] Y. H. Jo, M. H. Jung, M. C. Kyum, and S. I. Lee, J. Nanosci. Nanotechnol. **7**, 3884 (2007).
[14] K. Siemensmeyer, K. N. Clausen, K. Lefmann, O. V. Lounasmaa, A. Metz, K. K. Nummila, F. B. Rasmussen, M. Steiner, J. T. Tuoriniemi, and R. T. Vuorinen, Physica B **241**, 506 (1997).
[15] Y. Zhang, S. Talapatra, S. Kar, R. Vajtai, S. K. Nayak, and P. M. Ajayan, Phys. Rev. Lett. **99**, 107201 (2007).
[16] P. Esquinazi, D. Spemann, R. Höhne, A. Setzer, K. H. Han, and T. Butz, Phys. Rev. Lett. **91**, 227201 (2003).
[17] T. L. Makarova, Semiconductors **38**, 615 (2004).